Plant Phenomics 7 (2025) 100063

Contents lists available at ScienceDirect

Plant Phenomics

journal homepage: www.sciencedirect.com/journal/plant-phenomics

Research Article

Influence of fertilization on the dynamics of energy use in wheat☆

Xiuping Liu [a], Yunzhou Qiao [a], Zhenlin Tian [b,a], Heyong Liu [b], Hongliang Wu [a], Xiaoxin Li [a], Yuming Zhang [a], Chunsheng Hu [a], Wenxu Dong [a,*], Lianhong Gu [c,**]

[a] Hebei Key Laboratory of Soil Ecology, Center for Agricultural Resources Research, Institute of Genetics and Developmental Biology, Chinese Academy of Sciences, Shijiazhuang, 050021, China
[b] College of Life Sciences, Hebei University, Baoding, 071002, China
[c] Environmental Sciences Division and Climate Change Science Institute, Oak Ridge National Laboratory, Oak Ridge, TN, 37831, USA

ARTICLE INFO

Keywords:
Photosynthesis
Energy allocation
Photochemical compensation point
Leaf trait
Wheat

ABSTRACT

Plant energy use is fundamental to plant survival and growth. However, we still lack effective means to quantify plant energy use strategies. This study introduced a concept quantifying the light level at which photochemical and non-photochemical energy use in plants are in equilibrium — the photochemical compensation point (PCCP) which can be determined with chlorophyll fluorescence measurements. We used winter wheat as a test case to explore the dynamics of PCCP and its physiological and biochemical regulations. Winter wheat PCCP decreased significantly across growth stages from jointing to grain filling. Long-term nitrogen and phosphate (NP) fertilization significantly increased PCCP, whereas potassium (K) and manure (M) fertilizer supplementation had negligible effects. PCCP exhibited significant positive correlations with leaf thickness, leaf P and sulfur (S), and stomatal conductance (g_s) across all growth stages. All manure-amended treatments exhibited positive correlations of PCCP with leaf N, P, K and g_s, and negative correlations with leaf calcium (Ca). Random forest analysis revealed that g_s was the most significant predictor of PCCP variation, followed by leaf P, *iWUE*, and leaf thickness across all treatments. We suggest that plant energy use strategies are strongly coupled with plant water use strategies and nutrient availability through a complex interplay of effects on physiological and biochemical traits.

1. Introduction

Light is essential for plant growth and development [1]. Under normal light conditions, leaves utilize or dissipate absorbed light energy through processes such as photochemical quenching (PQ), chlorophyll fluorescence (ChlF), and non-photochemical quenching (NPQ) [2–4]. Because of the conservation of energy, these energy dissipation pathways compete for excitation energy; as a result, changes in one pathway are often correlated with energy dissipation in the others [5–7]. However, the relative energy allocations among the different pathways are dynamic and vary with species, growth stage, and environmental conditions [8,9]. Of particular importance is the partitioning of absorbed light energy in photosystem II (PSII) between the PQ and NPQ pathways, which reflects fundamental plant energy use strategies. Understanding plant energy use strategies is crucial to predicting photosynthetic responses to environmental variations.

Physically, the relative energy use by PQ and NPQ pathways depends on the rate constants of excitation energy transfer to reaction centers and dissipation as heat [10]. The precise values of these rate constants vary with the aggregation states of the antenna complexes, their coupling with reaction centers, properties of the electron transport chain, acidity of the lumen, and the dynamic structure of the thylakoid [8,9,11–14]. The biological mechanisms controlling these rate constants and therefore the relative energy use by the PQ and NPQ pathways in plants are

☆ This manuscript has been coauthored by UT-Battelle, LLC under Contract No. DE-AC05-00OR22725 with the US Department of Energy. The United States Government retains and the publisher, by accepting the article for publication, acknowledges that the United States Government retains a non-exclusive, paid-up, irrevocable, world-wide license to publish or reproduce the published form of this manuscript, or allow others to do so, for United States Government purposes. The Department of Energy will provide public access to these results of federally sponsored research in accordance with the DOE Public Access Plan (http://energy.gov/downloads/doe-public-access-plan).

* Corresponding author.
** Corresponding author.
E-mail addresses: dongwx@sjziam.ac.cn (W. Dong), lianhong-gu@ornl.gov (L. Gu).

https://doi.org/10.1016/j.plaphe.2025.100063
Received 24 December 2024; Received in revised form 10 May 2025; Accepted 1 June 2025
Available online 2 June 2025

complex and still under active research [15]. For example, multiple types of NPQ exist and each type is activated by different mechanisms and operates at different time scales with corresponding competition with PQ for excitation energy [16]. The operation of these biological mechanisms, however, ultimately depends on environmental conditions. Several studies have demonstrated that nitrogen (N) deficiency, compared to N replete controls, induces a decrease in carbon dioxide (CO_2) assimilation capacity, PQ and photochemical quantum yield of PSII (Φ_{PSII}) and an increase in NPQ in major agricultural crops such as wheat (*Triticum aestivum* L.), maize (*Zea mays* L.), and rice (*Oryza sativa* L.) [17–19]. Besides N, phosphorus (P) starvation induce lumen acidification, leading to an increase in NPQ, and a decrease in the photochemical dissipation of excitation energy from PSII [20,21]. In addition, stomata regulate CO_2 and water vapor diffusion from ambient air to leaf interior, and many photosynthetic parameters, including electron transport rate, respiration rate in the light, and steady-state chlorophyll fluorescence (F_s), are highly dependent on stomatal conductance (g_s) [22,23]. Furthermore, leaf intrinsic water use efficiency (*iWUE*), the ratio of net photosynthetic CO_2 assimilation rate (A_n) to g_s, has been demonstrated to be a key determinant of photosynthesis with strong correlation with CO_2 diffusion [24–26]. These findings suggest that plant energy use strategies are affected by soil nutrient availability which alters leaf physiological and biochemical traits (e.g., g_s, *iWUE*, and nutrient contents).

This study aims to gather insights into how plant photochemical vs non-photochemical energy use strategies are shaped by constraints in other crucial resources such as nutrients and water. We first demonstrate that the light level at which the photochemical energy use equals the non-photochemical energy use is a simple yet effective index for characterizing the plant energy use strategies. This index, which is termed the photochemical compensation point (PCCP, $\mu molm^{-2}s^{-1}$), is analogous to the long-established concepts of light compensation point [27] and CO_2 photocompensation point [28], and is expected to play a similarly significant role in photosynthesis research. We took advantage of a 23-year long-term integrated fertilization experiment of winter wheat-summer maize rotation in the North China Plain to evaluate the dynamics of PCCP. We performed combined measurements of ChlF and gas exchange of wheat across different fertilization treatments and growth stages, inferred the PCCP from fluorescence parameters and related them to leaf morphological, physiological, and developmental traits. We analyzed the data to answer the following questions: 1) How does the PCCP of wheat vary with growth stages under different long-term fertilization treatments? and 2) how do plant physiology and biochemistry regulate the PCCP of wheat? Understanding these two questions will lead to insights regarding plant energy use and how it is regulated.

2. Materials and methods

2.1. Energy allocation index

As light intensity increases under physiological conditions, the photochemical quantum yield of photosystem II (Φ_{PSII}) decreases while the corresponding non-photochemical quantum yield (Φ_{NPQ}) increases [29–33]. At some intermediate level of light intensity, the photochemical energy use equals the nonphotochemical energy use, and Φ_{PSII} and Φ_{NPQ} have the same value (Fig. 1). This photochemical-nonphotochemical equilibrium point is termed the PCCP. Below PCCP, more energy is used to drive electron transport than is actively dissipated as heat whereas above it, the opposite is true. Thus, PCCP represents a turning point in plant energy use. A high PCCP value will enable plants to utilize available sunlight more fully. However, this energy use strategy may run into an increased risk of photodamage, particularly when the capacity of plants to consume the products of electron transport (e.g., NADPH and ATP) is curtailed by environmental stresses such as drought, extreme temperatures and nutrient deficiencies. Thus we expect an optimal PCCP depends on prevailing environmental conditions, plant growth stages, and life history strategies [3,33–35]. For managed crops where environmental stresses are managed, a higher PCCP may be advantageous for crop yield. For plants in natural environments, it will be essential for plants to have a PCCP that balances photosynthetic efficiency and risks of photodamage. This expectation makes PCCP an interesting index to analyze for plant physiology.

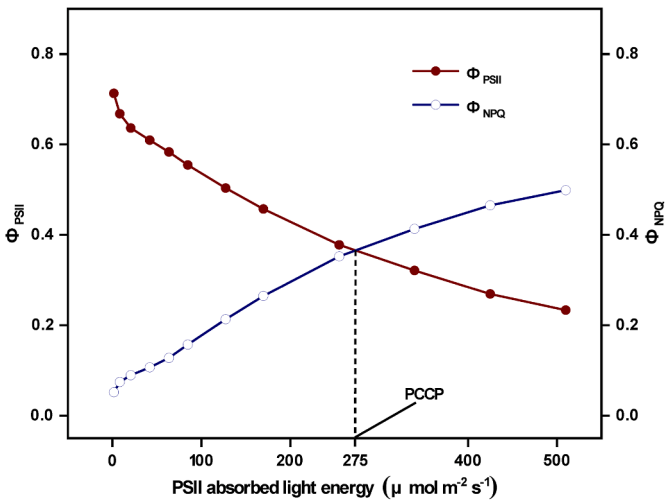

Fig. 1. A practical example of PCCP calculation. PCCP: photochemical compensation point; Φ_{PSII}: the fraction of absorbed light used for photochemistry; Φ_{NPQ}: the fraction of light quenched via dynamic NPQ.

2.2. Site description

The long-term field experiment was established in 2001 at the Luancheng Agroecosystem Experimental Station, Chinese Academy of Sciences (37° 53′ N, 114° 41′ E, elevation 50.1 m), located in Luancheng county, Hebei Province, China. The climate is warm, temperate semi-humid monsoon with cold winters and hot summers. The average annual precipitation for the period 1982–2021 is about 478.6 mm with a mean temperature of 12.6 °C. The soil of the area is an aquic cinnamon soil. Soil properties (0–20 cm) at the long-term fertilization site obtained in October 2022 were listed in Table 1.

The dominant cropping system in this region is winter wheat and summer maize rotation with no fallow in between. Summer maize is usually sown in June and harvested in early October, and winter wheat is sown in late October and harvested in early June the following year.

2.3. Experimental design

The long-term experiment was designed to test the effects of different fertilization strategies in a winter wheat (Kenong 2011) - summer maize (Zhengdan 958) cropping system. The experimental design consisted of ten treatments arranged in a randomized complete block design with three replications, resulting in a total of 30 plots each measuring 8 m × 16 m. For this study, eight fertilization treatments were selected in the winter wheat cropping system. The treatments were: (1) CK (no fertilizer); (2) N (inorganic N fertilizer); (3) NP (inorganic N and P fertilizer); (4): NPK (inorganic N, P, and K fertilizer); (5) M (manure); (6) NM (inorganic N fertilizer and manure); (7) NPM (inorganic N and P fertilizer and manure); (8) NPKM (inorganic N, P, and K fertilizer and manure). All treatments received the same fertilization rates: 300 kg ha^{-1} a^{-1} of N, 52.4 kg ha^{-1} a^{-1} of P, 62.6 kg ha^{-1} a^{-1} of K, and 6294 kg ha^{-1} a^{-1} of manure. N, P, and K fertilizer were supplied as urea (46 % N), superphosphate (12 % P_2O_5), and potassium chloride (60 % K_2O), respectively, with manure applied in dried pig manure. N fertilizer was applied annually in three split applications: 75 kg ha^{-1} as basal

Table 1
Characteristics of the topsoil (0–20 cm) sampled in October 2022 (mean ± S.E.).

Treatment	Organic matter (g kg^{-1})	Toal N (g kg^{-1})	Available N (mg kg^{-1})	Available P (mg kg^{-1})	Available K (mg kg^{-1})
CK	16.2 ± 0.05d	0.98 ± 0.02d	79.8 ± 1.76e	4.02 ± 0.44d	150 ± 12.5a
N	15.7 ± 0.03d	1.09 ± 0.02cd	105 ± 5.27d	4.50 ± 0.2d	140 ± 4.66a
NP	21.5 ± 0.37 ab	1.48 ± 0.06 ab	149 ± 3.64 ab	80.9 ± 5.7 ab	136 ± 17.4a
NPK	18.2 ± 0.98cd	1.28 ± 0.02bc	100 ± 2.77d	33.5 ± 5.32cd	175 ± 10.9a
M	20.6 ± 0.86bc	1.32 ± 0.04bc	114 ± 7.36cd	97.2 ± 9.49a	167 ± 3.72a
NM	19.4 ± 2.10bc	1.26 ± 0.16bc	113 ± 11.8cd	55.2 ± 6.93bc	170 ± 5.57a
NPM	24.3 ± 0.40a	1.63 ± 0.01a	152 ± 1.80a	88.8 ± 1.30 ab	159 ± 9.78a
NPKM	20.6 ± 1.41bc	1.38 ± 0.12b	129 ± 6.71bc	61.9 ± 8.01abc	179 ± 4.81a

CK: control without fertilizer; N: inorganic nitrogen fertilizer; NP: inorganic nitrogen and phosphate fertilizer; NPK: inorganic nitrogen, phosphate, and potassium fertilizer; M: manure; NM: inorganic nitrogen fertilizer and manure; NPM: inorganic nitrogen and phosphate fertilizer and manure; NPKM: inorganic nitrogen, phosphate, and potassium fertilizer and manure. S.E. stands for standard error. Different letters within columns indicate significant difference between treatments ($p < 0.05$).

Table 2
Application rates of mineral fertilizer and manure at the long-term fertilization site.

Treatment	Winter wheat					Summer maize	
	Basal				Supplement	Supplement	
	N (kg ha^{-1})	P (kg ha^{-1})	K (kg ha^{-1})	Manure (kg ha^{-1})	N (kg ha^{-1})	N (kg ha^{-1})	K (kg ha^{-1})
CK							
N	75				75	150	
NP	75	52.4			75	150	
NPK	75	52.4	31.3		75	150	31.3
M				6294			
NM	75			6294	75	150	
NPM	75	52.4		6294	75	150	
NPKM	75	52.4	31.3	6294	75	150	31.3

Fertilizer N, P, and K represent the content of pure N, P, and K, respectively. CK: control without fertilizer; N: inorganic nitrogen fertilizer; NP: inorganic nitrogen and phosphate fertilizer; NPK: inorganic nitrogen, phosphate, and potassium fertilizer; M: manure; NM: inorganic nitrogen fertilizer and manure; NPM: inorganic nitrogen and phosphate fertilizer and manure; NPKM: inorganic nitrogen, phosphate, and potassium fertilizer and manure.

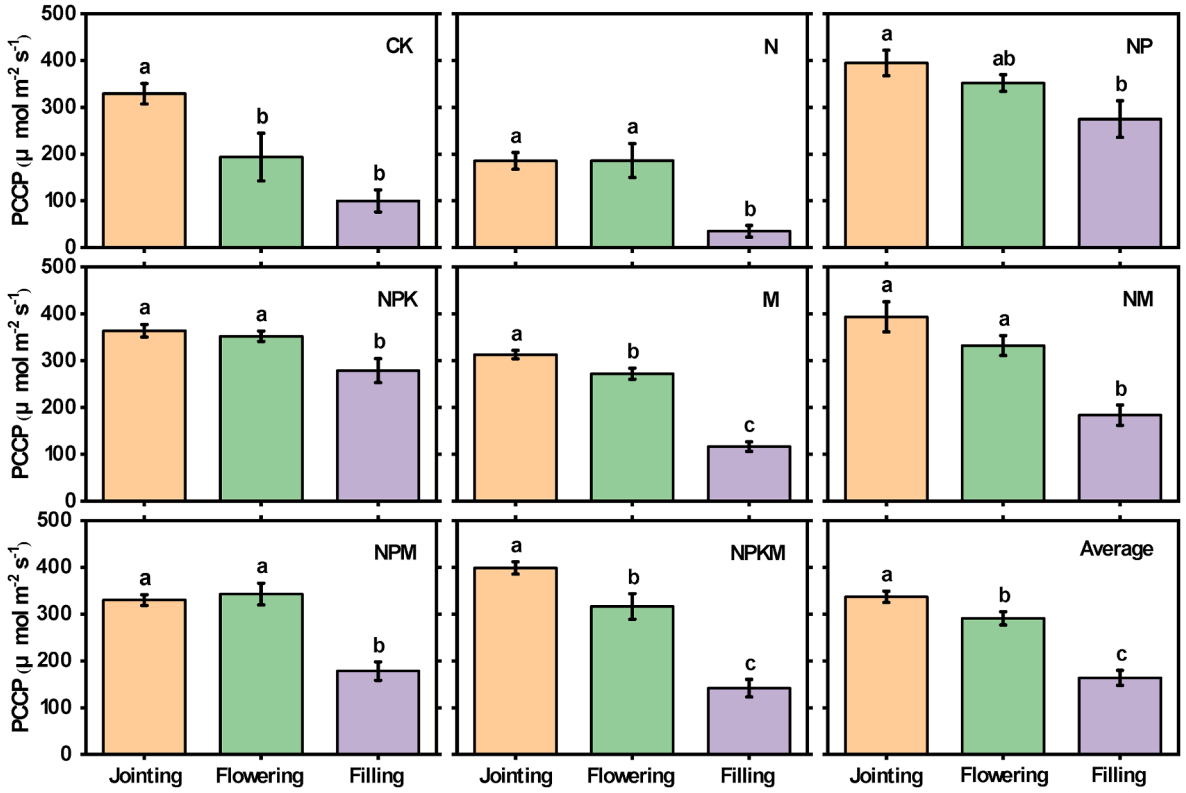

Fig. 2. The PCCP of wheat across different growth stages. PCCP: photochemical compensation point. Error bars represent standard errors. Different letters indicate significant difference between growth stages ($p < 0.05$).

fertilizer for wheat, 75 kg ha^{-1} as wheat topdressing, and 150 kg ha^{-1} as maize topdressing. P fertilizer and manure were applied as basal fertilizer for wheat. K fertilizer was applied twice a year, with half used as basal fertilizer for wheat and the other half as topdressing for maize. Base fertilizer was broadcast before wheat sowing, followed by rotary tillage and seeding. Topdressing was surface-applied at the jointing stage and immediately irrigated. For the two crops, the post-harvest straw was removed from the fields, with irrigation, herbicides, and pesticides applied as needed during the growing season. A detailed description of manure and inorganic fertilizers inputs were shown in Table 2.

2.4. Gas exchange and chlorophyll fluorescence measurements

During the 2023 and 2024 wheat growing seasons, simultaneous light response curves of gas exchange and ChlF were measured on fully expanded top leaves at the jointing, flowering, and filling stages. Dark-adapted minimum and maximum fluorescence (F_o and F_m, respectively) were measured before dawn using a LI-6400XT photosynthesis system equipped with a LI-6400-40 leaf chamber fluorometer (Li-Cor, Lincoln, NE, USA). The rest measurements were performed between 9:00 and 16:00. For production of light response curves, leaves were adapted to 400 μmol mol^{-1} CO_2, 1200 μmol m^{-2} s^{-1} photosynthetically active radiation (PAR), 500 μmol s^{-1} airflow, and ambient temperature and relative humidity until A_n and g_s were stable. Measurements of light-adapted steady-state (F_s) and maximum (F'_m) fluorescence were made at successively decreasing light intensities (1200, 1000, 800, 600, 400, 300, 200, 150, 100, 50, 20, and 0 μmol m^{-2} s^{-1}). Prior to each recording, leaves were acclimated to each PAR level for 2–4 min, after which CO_2 and H_2O concentrations of sample cell and reference cell were automatically matched. Four replicate measurements per treatment yielded 122 wheat light response curves.

Φ_{PSII} and Φ_{NPQ} were calculated using $\frac{F'_m-F_s}{F'_m}$ and $\frac{F_s}{F'_m}-\frac{F_s}{F_m}$ [36,37], respectively, and absorbed light energy by PSII was calculated as $\alpha\beta \times$ PAR, where F_s is the fluorescence emission yield from light-adapted leaves at steady-state, F'_m is the maximal fluorescence from light-adapted leaves, F_m is the maximal fluorescence from dark-adapted leaves, PAR (μmol m^{-2} s^{-1}) is the incident photosynthetically active radiation, $\alpha = 0.85$ is the leaf absorptance in PAR, and $\beta = 0.5$ is the fraction of absorbed PAR allocated to PSII. Linear interpolation of measured Φ_{PSII} and Φ_{NPQ} values at varying PSII light absorption levels yielded light response curves. The light intensity at their intersection

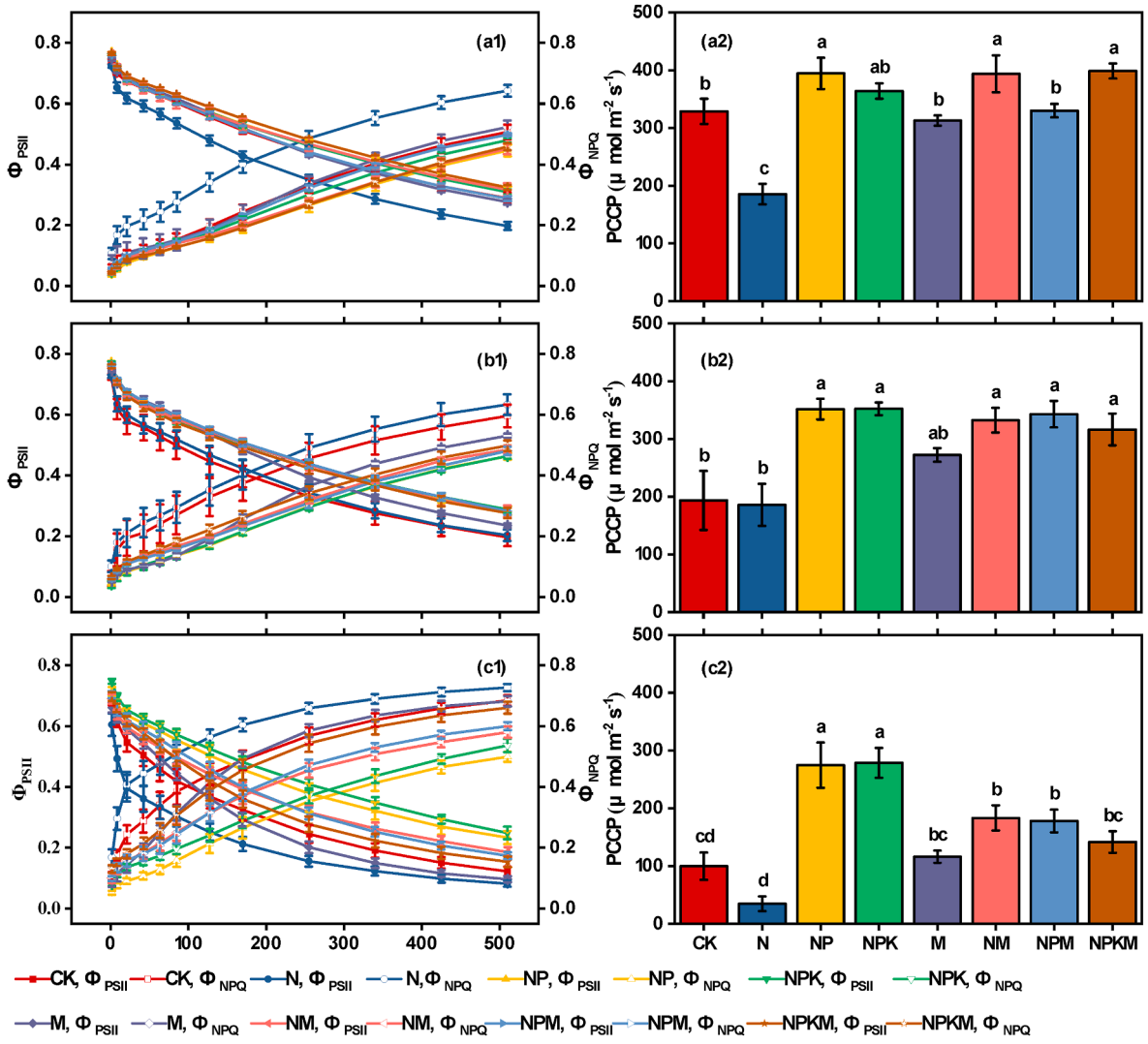

Fig. 3. Φ_{PSII} and Φ_{NPQ} light response curves and PCCP of wheat across different fertilization treatments. PCCP: photochemical compensation point; Φ_{PSII}: the fraction of absorbed light used for photochemistry; Φ_{NPQ}: the fraction of light quenched via dynamic NPQ. Error bars represent standard errors. a1 and a2: jointing; b1 and b2: flowering; c1 and c2: filling. Different letters indicate significant difference between treatments ($p < 0.05$).

represented the PCCP (Fig. 1). Data interpolation and PCCP point calculation were performed using NumPy [38].

2.5. Leaf traits

After gas exchange measurements, all leaves were collected, leaf area (using an electronic area meter, LI-3000A, Li-Cor, Lincoln, NE), leaf thickness (using a digital micrometer, Mitutoyo, Japan) and leaf dry mass (after drying at 60 °C to constant mass) were measured, and specific leaf weight was calculated as the ratio of leaf dry mass to leaf area. Subsequently, dried leaf samples were ground and analyzed for N content by Kjeldahl method (Kjeltec 8400, Foss, Sweden), P content by molybdate colorimetric method (UV-2450, Shimadzu, Japan), K content by flame atomic absorption spectrophotometer (Analytik Jena, Germany) and calcium (Ca), iron (Fe), and sulfur (S) content by inductively coupled plasma spectrometer (iCAP PRO, Thermo Fisher, Germany).

g_s and *iWUE* were calculated under a light intensity of 1200 μmol m^{-2} s^{-1}. *iWUE* was calculated as A_n/g_s, where A_n (μmol m^{-2} s^{-1}) is the net photosynthetic CO_2 assimilation rate, and g_s (mol m^{-2} s^{-1}) is the stomatal conductance, both of which were measured using the LI-6400XT photosynthesis system.

Thus, a total of ten leaf traits were quantified: leaf thickness, specific leaf weight, leaf N, P, K, Ca, Fe, and S contents, g_s, and *iWUE*.

2.6. Statistical analyses

Kolmogorov–Smirnov test was used to check the data distribution, and data were transformed to normal for one-way analysis of variance (ANOVA) when necessary. ANOVA followed by least significant difference (LSD) multiple comparison ($p < 0.05$) was used to assess the differences in PCCP between treatments at different growth stages. Linear and nonlinear regression models were employed to evaluate the relationship between PCCP and leaf traits across fertilization treatments and growth stages, as well as the link between stage-specific PCCP and final grain yield. The model with the highest coefficient of determination (R^2) was selected. Random forest analysis was performed using the rfPermute and A3 packages to assess the relative importance of leaf traits on PCCP [39], with each variable's importance expressed as the increase in mean

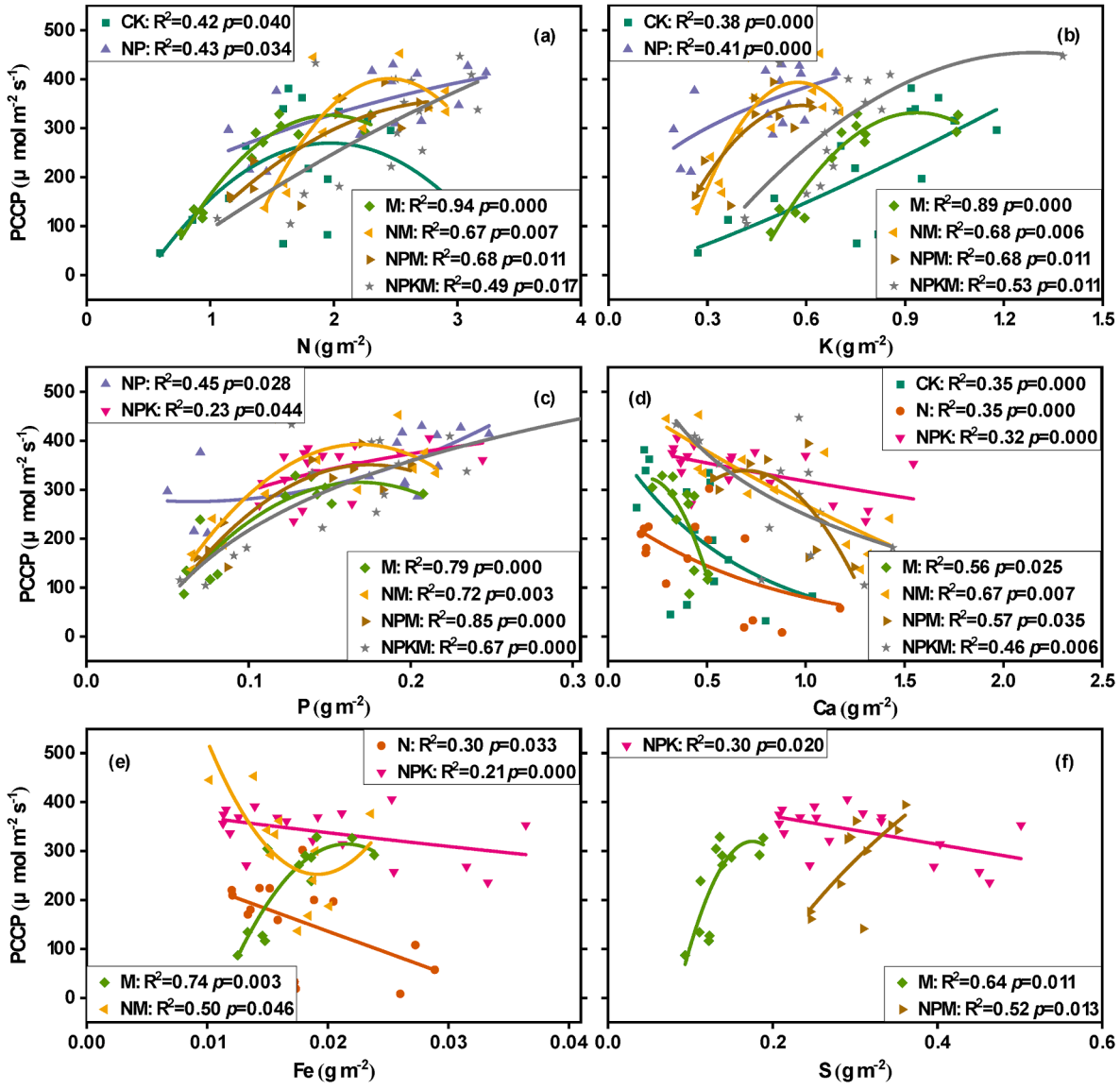

Fig. 4. Relationship between PCCP and leaf biochemical traits across fertilization treatments. a: PCCP vs. leaf N; b: PCCP vs. leaf P; c: PCCP vs. leaf K; d: PCCP vs. leaf Ca; e: PCCP vs. leaf Fe; f: PCCP vs. leaf S. Fertilization treatments: CK (jungle green squares); N (burnt orange circles); NP (slate blue upward triangles); NPK (razzmatazz downward triangles); M (lime green diamonds); NM (goldenrod left triangles); NPM (golden brown right triangles); NPKM (dim gray stars). PCCP: photochemical compensation point.

squared error (IncMSE) value. To improve prediction accuracy, a full random forest model was first constructed by incorporating all collected variables into the algorithm. Subsequently, the identified significant variables mentioned above were selected and randomly dropped to develop a more accurate sparse model. Prior to constructing the sparse model, ten-fold cross-validation with 10 repetitions was conducted to determine the optimal number of variables to include. During each repetition, the dataset was randomly split into 10 subsets, with nine used for training and one for testing. The optimal number of variables was selected based on the cross-validation error. PCCP was calculated in Anaconda version 3, ANOVA analyses were performed using SPSS 19 for Windows, and random forest analysis was conducted in R version 4.3.3.

3. Results

3.1. Temporal dynamics of PCCP

Daily mean PCCP of wheat averaged 272 ± 10.3 μmol m^{-2} s^{-1} from 2023 to 2024 (Fig. 2). Throughout the growing season, daily PCCP decreased significantly from 337 ± 12.3 μmol m^{-2} s^{-1} at jointing to 291 ± 14.3 μmol m^{-2} s^{-1} at flowering, and then to 163 ± 15.9 μmol m^{-2} s^{-1} at filling (Fig. 2). A significant reduction in PCCP was observed at filling compared to the jointing and flowering (except for CK and NP at flowering) (Fig. 2). However, with the exception of CK, M, and NPKM treatments, the difference in PCCP between the jointing and flowering was not significant (Fig. 2). PCCP significantly decreased across growth stages, particularly at filling.

3.2. Variations of PCCP between treatments

Long-term different fertilization significantly influenced the PCCP of wheat (Fig. 3). Among all the treatments, the PCCP was highest in NP and NPK (NPKM at jointing) and lowest in the N treatment (Fig. 3). Compared with CK, N and M application did not significantly increase or even decrease the PCCP, whereas combined N and M application significantly increased the PCCP (Fig. 3). PCCP in NP, NPK, NPM, and NPKM treatments was significantly higher than control (except NPM at jointing and NPKM at filling), while there was no significant difference between NP and NPK and between NP and NPM, and NPM application even decreased the PCCP at jointing and filling stages (Fig. 3). Long-term NP fertilization significantly increased wheat PCCP, whereas K and M supplementation had little effect on the PCCP.

3.3. Variations of PCCP with leaf traits

Fertilization regimes significantly influenced the relationship between PCCP and leaf biochemical traits (Fig. 4). PCCP was positively correlated with leaf N and K under CK and NP treatments, and with leaf P under NP and NPK treatments (Fig. 4a–c). In contrast, it was consistently negatively correlated with leaf Ca under CK, N, and NPK treatments (Fig. 4d). All manure-amended treatments (M, NM, NPM, NPKM) exhibited positive correlations of PCCP with leaf N, P and K, and negative with leaf Ca (Fig. 4a–d), with manure addition enhancing these relationships. For micronutrients, PCCP correlated negatively with Fe under N, NPK, and NM but positively under M, whereas its correlation with S was negative under NPK and turned positive under both M and NPM (Fig. 4e and f). Regarding leaf physiological traits (Fig. 5), PCCP correlated positively with g_s in all treatments except NP and NPK (Fig. 5a), and with leaf thickness in NP, NM, NPM and NPKM (Fig. 5b). It was also positively related to *iWUE* under N, NP, and M but negatively under NPM (Fig. 5c), and showed no significant relationship with specific leaf weight ($p > 0.05$).

Beyond fertilization effects, PCCP also exhibited dynamic relationships with leaf biochemical traits during wheat growth (Fig. 6). Specifically, strong positive correlations were observed with leaf P across all growth stages (Fig. 6a). A weak but statistically significant positive correlation was also found with leaf S (Fig. 6b). Leaf N and K exhibited complex stage-dependent relationships, showing positive and negative correlations respectively at jointing, but a consistent positive correlation across the entire season (Fig. 6c and d). Similarly, the positive correlation between PCCP and leaf Ca was stage-specific (jointing, flowering, and grain filling, Fig. 6e), unlike the consistent positive relationship with leaf Fe observed only during grain filling (Fig. 6f). Regarding the effects of leaf physiological traits on PCCP, significant positive correlations were found with leaf thickness and g_s across all growth stages (Fig. 7a and b). No significant correlation was observed with specific leaf weight ($p > 0.05$). PCCP displayed a significant positive correlation with *iWUE* during grain filling and across the entire growing season (Fig. 7c).

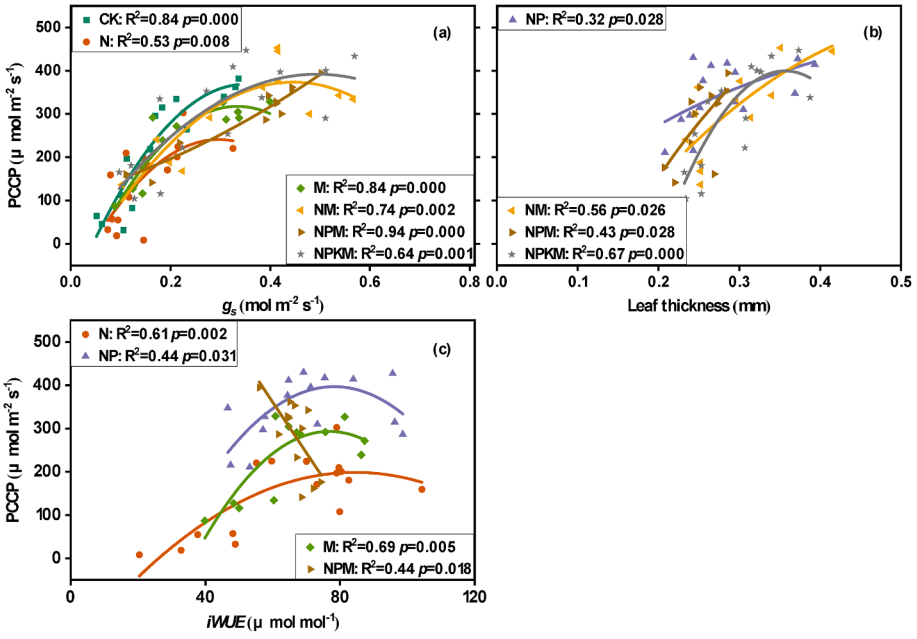

Fig. 5. Relationship between PCCP and leaf physiological traits across fertilization treatments. a: PCCP vs. g_s; b: PCCP vs. leaf thickness; c: PCCP vs. *iWUE*. Fertilization treatments: CK (jungle green squares); N (burnt orange circles); NP (slate blue upward triangles); NPK (razzmatazz downward triangles); M (lime green diamonds); NM (goldenrod left triangles); NPM (golden brown right triangles); NPKM (dim gray stars). PCCP: photochemical compensation point g_s: stomatal conductance; *iWUE*: intrinsic water use efficiency.

3.4. Potential drivers of PCCP

The full random forest model explained 75.5 % of the variation in PCCP (Fig. 8). Six significant predictors were identified, of which g_s was the most important (IncMSE = 30.2 %), followed by leaf P (16.5 %), *iWUE* (11.9 %), leaf thickness (11.0 %), leaf N (7.37 %), and leaf K (6.45 %) (Fig. 8a). Based on the results, sparse random forest model was built using the significant variables identified above, and it explained 77.6 % of the total variation (Fig. 8b). Ten-fold cross-validation indicated that the model achieved the lowest cross-validation error with four variables. As a result, we excluded the insignificant variables to enhance the model's robustness. The final optimized model included g_s, leaf P, *iWUE*, and leaf thickness as predictors, accounting for 76.8 % of the total variations (Fig. 8b).

4. Discussion

To our knowledge, this is the first time that the concept of PCCP is introduced so no previous study existed for direct comparison. Nevertheless, relevant studies provide context for the importance and usefulness of PCCP and for the findings of the present study. Light energy absorbed by PSII is allocated to either photochemistry, thermal dissipation or chlorophyll fluorescence [40]. Several studies have reported energy allocation and its response to environmental conditions [41,42]. For example, Ishida et al. [3] and Endo et al. [6] revealed that Φ_{PSII} responded very rapidly to sudden fluctuations of PAR, accompanied by an inverse change in Φ_{NPQ}. Chen et al. [40] and Hendrickson et al. [43] concluded that, under high light conditions, most absorbed light energy is consumed via thermal dissipation, with only a small proportion used for photochemistry. Conversely, under low light or non-stress conditions, most light energy was utilized for photochemistry, with smaller amounts of energy allocated to thermal dissipation [2,3]. Despite extensive research into the connection between plant photochemical and non-photochemical energy use [33,44], the scenarios where light energy converted to photochemistry is equal to energy dissipated as heat have received limited attention. This study introduced the PCCP, an indicator of plant energy allocation strategy, and investigated its dynamics and regulation in wheat under long-term fertilization regimes.

ChlF has been widely validated as a robust proxy for quantifying photosynthetic activity across plant species [2,42]. For example,

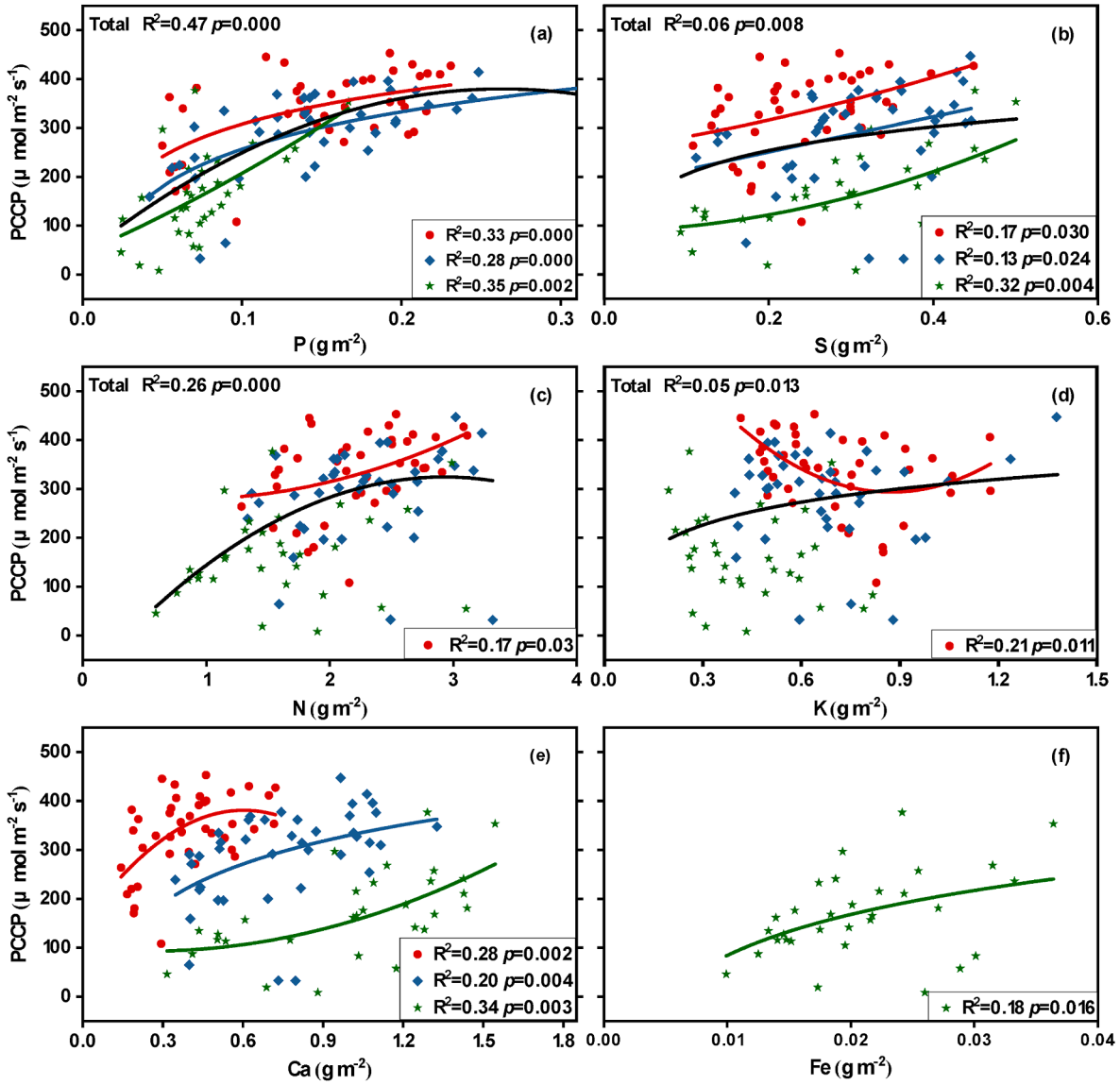

Fig. 6. Relationship between PCCP and leaf biochemical traits across growth stages. a: PCCP vs. leaf P; b: PCCP vs. leaf S; c: PCCP vs. leaf N; d: PCCP vs. leaf K; e: PCCP vs. leaf Ca; f: PCCP vs. leaf Fe. Red circles and lines denote the jointing stage, blue diamonds and lines the flowering stage, green stars and lines the filling stage, while black lines span the entire growing season. PCCP: photochemical compensation point.

Cendrero-Mateo et al. [5] demonstrated a strong positive correlation between CO_2 assimilation rate and ChlF in *Camelina sativa* leaves, while Sherstneva et al. [42] further highlighted the predictive value of ChlF-derived parameters (e.g., PSII effective quantum yield) for wheat biomass accumulation. Although conventional fluorescence parameters (e.g., Φ_{PSII} and Φ_{NPQ}) effectively capture instantaneous photochemical efficiencies at the leaf level, they fall short of delivering an integrated quantitative index for plant energy-allocation trade-offs [45]. In contrast, PCCP integrates dynamic interactions between photochemical processes and thermal dissipation, thereby providing a mechanistic link to actual carbon allocation towards grain development rather than transient leaf-level energy dynamics. The strong temporal correlation between stage-specific PCCP and final grain yield (Fig. 9) highlighted its superior predictive capacity over static fluorescence parameters. As the first evidence linking PCCP—a key photophysiological trait—to wheat yield formation, this study revealed its consistent regulatory role in photosynthetic carbon partitioning and grain filling across developmental stages.

Research has highlighted coordinated changes in Φ_{PSII} and Φ_{NPQ} across different seasons [3,34,46]. For example, Ishida et al. [3] reported that Φ_{PSII} in the growing season was greater than that in the ripening season, and the seasonal decline in PSII performance was accompanied by an inverse increase in Φ_{NPQ}. In line with these findings, this study found that as wheat plants mature, PSII increasingly dissipated light energy as heat rather than utilizing it for photochemistry. Similar to Φ_{PSII}, the PCCP of wheat also progressively declined with plant maturity, indicating a dynamic regulatory mechanism for light energy utilization across different developmental stages. Ishida et al. [3] speculated that the lower Φ_{PSII} at ripening, compared to the growing stage, may be due to more severe afternoon suppression of Φ_{PSII} in that phase. Maseyk et al. [34] stated that low g_s in summer reduced net CO_2 assimilation rates and increased the proportion of photochemical energy directed to non-assimilatory electron sinks. However, Knoblauch and Peters [47] suggested that the translocation of photosynthates from leaf sheaths during the vegetative phase to the panicles during the reproductive stage could account for this phenomenon. This emphasized the complex interplay of environmental and physiological factors that influence the balance between light energy utilization and dissipation in plants.

Our study investigated how fertilization modified PCCP in wheat plants. Previous studies have reported that N deficiency can significantly impact PSII photochemistry, reducing Φ_{PSII} while increasing NPQ [19,48,49]. However, our results showed that N application alone had no significant effects on PCCP values compared with control. Moreover, PCCP was not always significantly correlated with leaf N content. These findings aligned with those of Shrestha et al. [35] and Vijayalakshmi et al. [50], suggesting that N application did not always affect PSII photochemical efficiency and excitation energy partitioning among the three processes [35,51]. Unlike N, P has been shown to have a significant impact on PSII photochemistry [52–55]. Our results supported these findings, throughout the entire growing season, PCCP was positively correlated with leaf P content. This indicated that plants that received sufficient P nutrition exhibited higher PSII performance, more efficient energy capture and less energy dissipation as heat or fluorescence [20,21,56,57]. However, there are several conflicting reports regarding the effects of K levels on PSII photochemistry. Jákli et al. [58] reported that K deficiency significantly reduced Φ_{PSII} and enhanced NPQ in sunflower leaves, whereas Yang et al. [59] showed that Φ_{PSII} first increased and then decreased with increasing K content in the nutrient solution, accompanied by a reverse change in NPQ. The current results did not show considerable change in PCCP with K supplementation. Hence it is a great challenge to determine how PCCP change with K

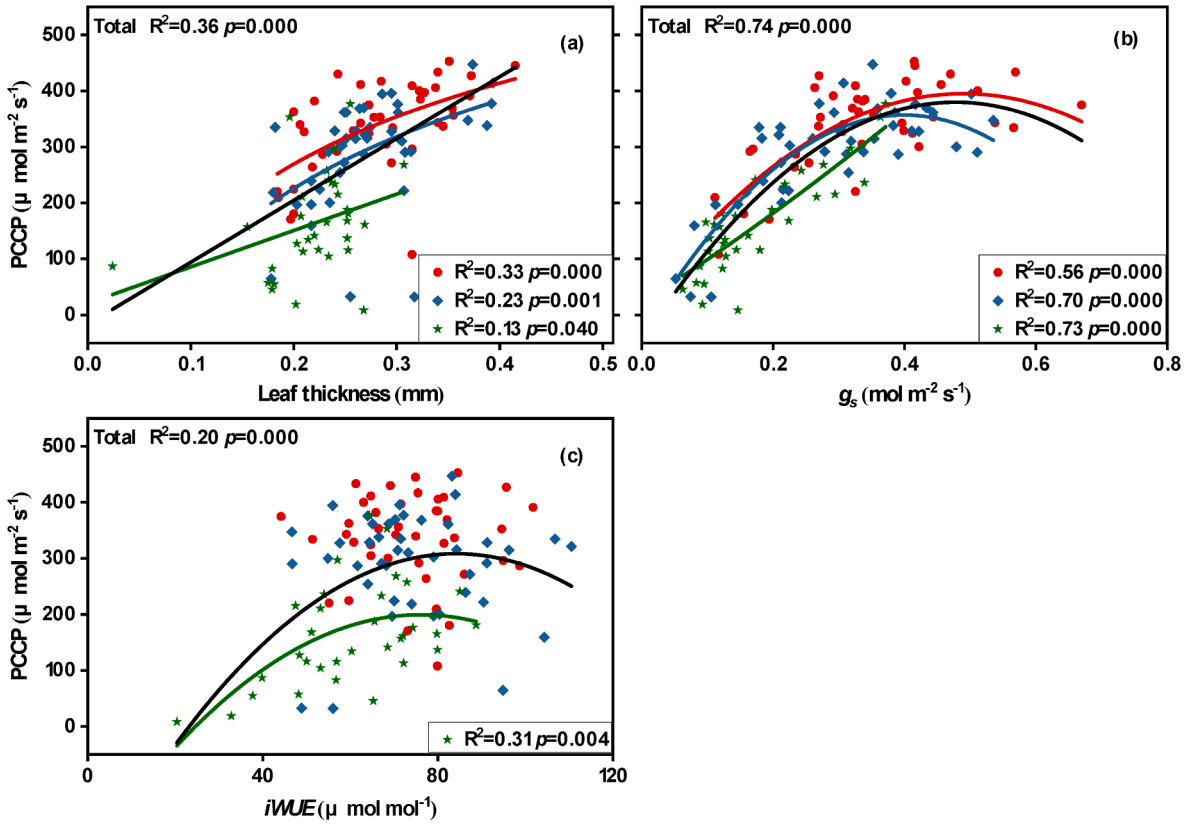

Fig. 7. Relationship between PCCP and leaf physiological traits across growth stages. a: PCCP vs. leaf thickness; b: PCCP vs. g_s; c: PCCP vs. *iWUE*. Red circles and lines denote the jointing stage, blue diamonds and lines the flowering stage, green stars and lines the filling stage, while black lines span the entire growing season. PCCP: photochemical compensation point. g_s: stomatal conductance; *iWUE*: intrinsic water use efficiency.

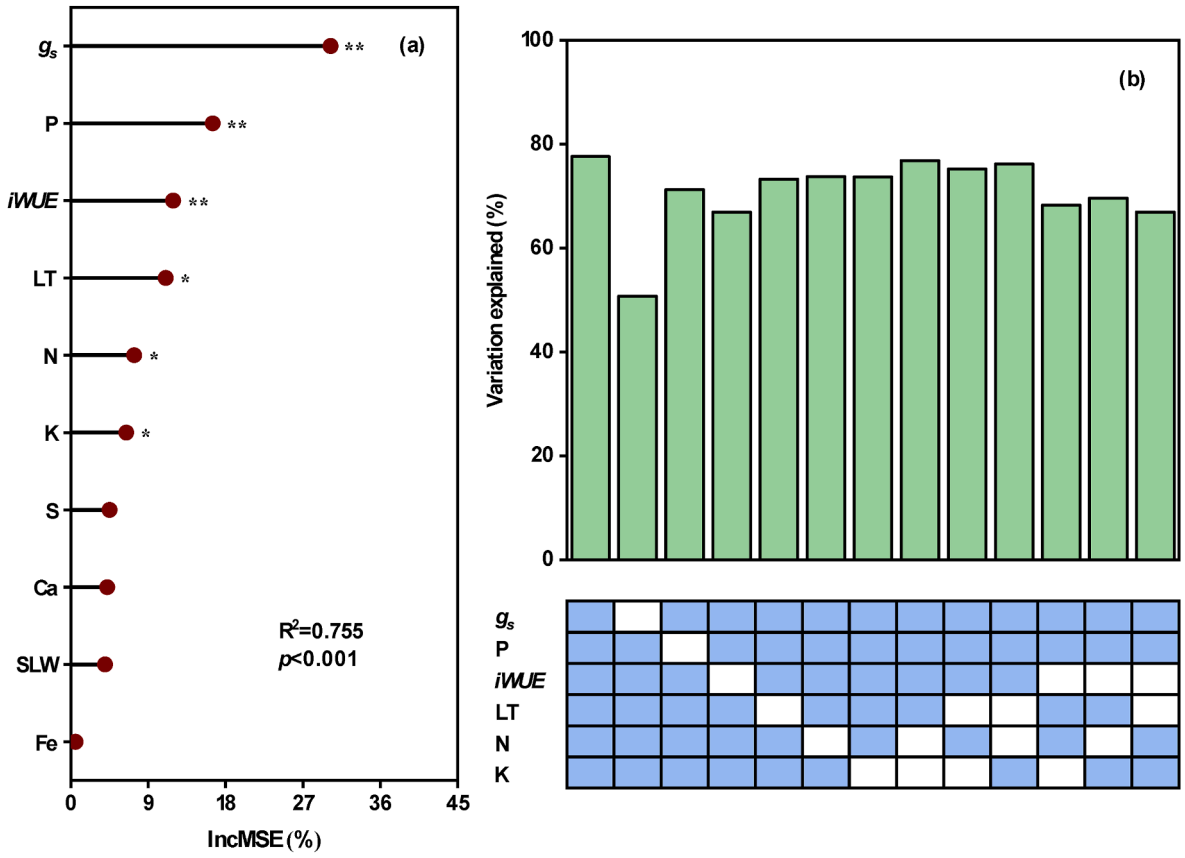

Fig. 8. Full (a) and sparse (b) models of random forest analysis predicting the effect of leaf characteristics on PCCP. IncMSE of variables in Fig. a were used to estimate the importance of these predictors, with higher MSE% values indicating more important predictors. The bar graph in Fig. b illustrated the explanation of photochemical compensation point for each sparse model, with colored boxes beneath each bar indicating the left-listed variables were included in the model, and the empty boxes indicating the variables were not included. LT: leaf thickness; SLW: specific leaf weight; g_s: stomatal conductance; *iWUE*: intrinsic water use efficiency; IncMSE: increases in the mean squared error. Significant factors were marked with an asterisk. *, $p < 0.05$, **, $p < 0.01$.

fertilization without affecting photosynthetic related traits. In addition, the observed greater PCCP in thicker leaves was consistent with previous findings. Thicker leaves exhibited greater photosynthetic activity due to increased palisade tissue, higher chlorophyll content, and improved light capture [60,61]. This was further supported by Li et al. [62], who demonstrated the role of leaf thickness in modulating light-induced anthocyanin synthesis and subsequent energy absorption, utilization, and allocation. Furthermore, nutrient addition improved stomatal traits, facilitating greater CO_2 uptake and light energy capture, ultimately leading to enhanced photosynthetic efficiency [23,63,64]. Our results showed that PCCP increased with g_s as wheat grew. However, according to Jacob and Lawlor [65], the reduced photosynthetic capacity of P deficient leaves is primarily attributed to limitations in mesophyll processes, rather than g_s or CO_2 diffusion. These observed complex interactions between nutrient levels, leaf structure, and PCCP highlight the need for further research to unravel the underlying mechanisms driving PCCP variation.

Under natural conditions, light energy allocation in PSII is not determined by a single factor, but by a complex interplay of internal and external factors related to leaf. Random forest analysis identified g_s, leaf P, *iWUE*, and leaf thickness as key drivers of PCCP among all leaf traits considered with g_s as the most important. These factors, particularly leaf P and leaf thickness, were strongly influenced by nutrient availability, allowing plants to adapt their morphology and physiology to improve light energy capture and allocation [66,67]. Studies of leaf structure, nutrient availability, and photosynthesis revealed that leaf N, leaf thickness, and amount of mesophyll per unit leaf area were the factors best explaining the variation in CO_2 assimilation rate [60]. Meanwhile,

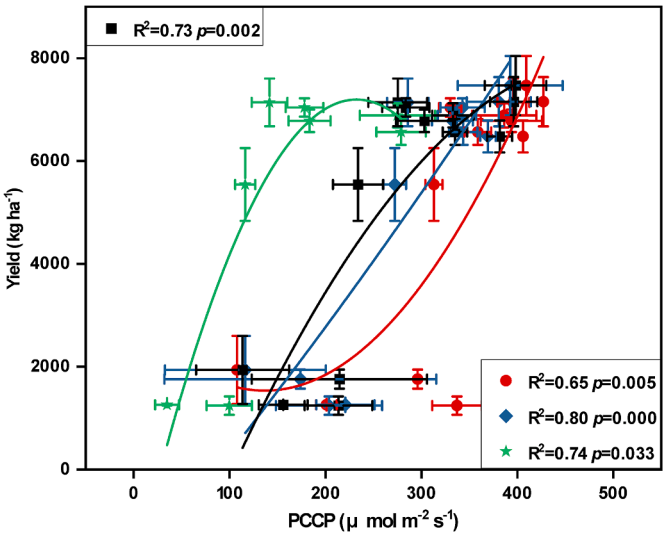

Fig. 9. Yield response to PCCP variations across growth stages (means of respective treatments). Growth stage: jointing (red circles); flowering (blue diamonds); filling (green stars); full season (black squares). PCCP: photochemical compensation point.

Wang et al. [68] indicated that adding P or NP fertilizers enhanced stomatal functions, such as g_s, *iWUE*, and stomatal slope parameters, which contributed to increased photosynthetic capacity in *Elymus*

dahuricus and *Gentiana straminea*. Nevertheless, according to Zheng et al. [69], excessively high CO_2 fertilization reduced N availability and g_s, leading to down-regulation of photochemical process, and this down-regulation is further influenced by water stress [70]. These findings reinforced the intricate interplay of leaf traits, nutrient availability, and environmental factors in optimizing light energy allocation in PSII and ultimately enhancing photosynthetic efficiency.

Besides indicating metabolic equilibrium, PCCP serves as an ecophysiological benchmark reflecting interspecific differences in photoprotective acclimation among genotypes and across environmental gradients [71]. Elevated PCCP values extend the irradiance range where photochemistry prevails over protective dissipation, thereby enhancing photosynthetic productivity while mitigating photodamage risks [3,34]. This dual functionality establishes PCCP as a pivotal indicator of the evolutionary trade-off between photosynthetic carbon assimilation and photoprotective metabolic costs. Notably, PCCP demonstrates environmental plasticity, with its optimal levels being modulated by species-specific life history strategies, developmental stages, and environmental parameters [33,35]. Such context-dependent adaptability positions PCCP as a compelling diagnostic tool for plant physiological studies aimed at optimizing photosynthetic performance under dynamic light conditions.

5. Conclusion

This study introduced the concept of PCCP and explored its dynamics and potential drivers in wheat. Wheat PCCP averaged 272 μmol m^{-2} s^{-1}, significantly decreasing from 337 μmol m^{-2} s^{-1} at jointing to 163 μmol m^{-2} s^{-1} at late grain filling. Long-term NP fertilization significantly increased the PCCP of wheat, whereas K and M fertilizer supplementation had negligible effects. Wheat PCCP exhibited significant positive correlations with leaf thickness, leaf P and S, and g_s across all growth stages. All manure-amended treatments exhibited positive correlations of PCCP with leaf N, P, K and g_s, and negative with leaf calcium (Ca). Random forest analysis revealed that g_s was the most significant predictor of PCCP variation, followed by leaf P, *iWUE*, and leaf thickness across all treatments. The strong relationship between PCCP and g_s points to an intimate coupling between plant energy and water use strategies. Long-term fertilization altered wheat energy use strategies through a complex interplay of effects on physiological and biochemical traits across different growth stages.

Author contributions

C.H. and L.G. conceived and guided the experiments. X.L. and Z.T. performed the experiments. X.L. and L.G. wrote the manuscript. C.H. and W.D. supervised the project. Y.Q., H.L., H.W., X.X.L., and Y.Z. revised and finalized the manuscript.

Data availability

Data will be made available on request.

Declaration of competing interest

The authors declare that they have no known competing financial interests or personal relationships that could have appeared to influence the work reported in this paper.

Acknowledgments

This research was supported by the National Key Research and Development Program of China (2021YFD1901104, 2022YFD1901604), the “Strategic Priority Research Program” of the Chinese Academy of Sciences (XDA28020303, XDA26040103), and the Key Research and Development Program of Hebei Province (22326410D, 22326412D). LG is supported by the U.S. Department of Energy (DOE), Office of Science, Biological and Environmental Research Program. ORNL is managed by UT-Battelle, LLC, for DOE under contract DE-AC05-00OR22725.

References

[1] C. Miyake, K. Amako, N. Shiraishi, T. Sugimoto, Acclimation of tobacco leaves to high light intensity drives the plastoquinone oxidation system—relationship among the fraction of open PSII centers, non-photochemical quenching of Chl fluorescence and the maximum quantum yield of PSII in the dark, Plant Cell Physiol. 50 (2009) 730–743.
[2] X. Chen, X. Mo, S. Hu, S. Liu, Relationship between fluorescence yield and photochemical yield under water stress and intermediate light conditions, J. Exp. Bot. 70 (2019) 301–313.
[3] S. Ishida, N. Uebayashi, Y. Tazoe, M. Ikeuchi, K. Homma, F. Sato, T. Endo, Diurnal and developmental changes in energy allocation of absorbed light at PSII in field-grown rice, Plant Cell Physiol. 55 (2014) 171–182.
[4] A. Kanazawa, A. Chattopadhyay, S. Kuhlgert, H. Tuitupou, T. Maiti, D.M. Kramer, Light potentials of photosynthetic energy storage in the field: what limits the ability to use or dissipate rapidly increased light energy? R. Soc. Open Sci. 8 (2021) 211102.
[5] M.P. Cendrero-Mateo, A.E. Carmo-Silva, A. Porcar-Castell, E.P. Hamerlynck, S. A. Papuga, M.S. Moran, Dynamic response of plant chlorophyll fluorescence to light, water and nutrient availability, Funct. Plant Biol. 42 (2015) 746–757.
[6] T. Endo, N. Uebayashi, S. Ishida, M. Ikeuchi, F. Sato, Light energy allocation at PSII under field light conditions: how much energy is lost in NPQ-associated dissipation? Plant Physiol. Biochem. (Issy les Moulineaux, Fr.) 81 (2014) 115–120.
[7] W. Han, X.W. Xu, L. Li, J.Q. Lei, S.Y. Li, Chlorophyll a fluorescence responses of *Haloxylon ammodendron* seedlings subjected to progressive saline stress in the Tarim desert highway ecological shelterbelt, Photosynthetica 48 (2010) 635–640.
[8] C. Chen, D. Zhang, P. Li, F. Ma, Partitioning of absorbed light energy differed between the sun-exposed side and the shaded side of apple fruits under high light conditions, Plant Physiol. Biochem. (Issy les Moulineaux, Fr.) 60 (2012) 12–17.
[9] A. Porcar-Castell, J.I. Garcia-Plazaola, C.J. Nichol, P. Kolari, B. Olascoaga, N. Kuusinen, B. Fernández-Marín, M. Pulkkinen, E. Juurola, E. Nikinmaa, Physiology of the seasonal relationship between the photochemical reflectance index and photosynthetic light use efficiency, Oecologia 170 (2012) 313–323.
[10] L. Gu, J. Han, J.D. Wood, C.Y. Chang, Y. Sun, Sun-induced Chl fluorescence and its importance for biophysical modeling of photosynthesis based on light reactions, New Phytol. 223 (2019) 1179–1191.
[11] Y. Tang, X. Wen, Q. Lu, Z. Yang, Z. Cheng, C. Lu, Heat stress induces an aggregation of the light-harvesting complex of photosystem II in spinach plants, Plant Physiol. 143 (2007) 629–638.
[12] L. Nicol, W.J. Nawrocki, R. Croce, Disentangling the sites of non-photochemical quenching in vascular plants, Nat. Plants 11 (2019) 1177–1183.
[13] L. Gu, B. Grodzinski, J. Han, T. Marie, Y.-J. Zhang, Y.C. Song, Y. Sun, Granal thylakoid structure and function: explaining an enduring mystery of higher plants, New Phytol. 236 (2022) 319–329.
[14] L. Gu, B. Grodzinski, J. Han, T. Marie, Y.-J. Zhang, Y.C. Song, Y. Sun, An exploratory steady-state redox model of photosynthetic linear electron transport for use in complete modeling of photosynthesis for broad applications, Plant Cell Environ. 46 (2023) 1540–1561.
[15] C.J. Steen, J.M. Morris, A.H. Short, K.K. Niyogi, G.R. Fleming, Complex roles of PsbS and xanthophylls in the regulation of nonphotochemical quenching in *Arabidopsis thaliana* under fluctuating Light, J. Phys. Chem. B 124 (2020) 10311–10325.
[16] G. Zuo, Non-photochemical quenching (NPQ) in photoprotection: insights into NPQ levels required to avoid photoinactivation and photoinhibition, New Phytol. 246 (2025) 1967–1974.
[17] L. Cabrera-Bosquet, R. Albrizio, J.L. Araus, S. Nogués, Photosynthetic capacity of field-grown durum wheat under different N availabilities: a comparative study from leaf to canopy, Environ. Exp. Bot. 67 (2009) 145–152.
[18] E. Kumagai, T. Araki, O. Ueno, Comparison of susceptibility to photoinhibition and energy partitioning of absorbed light in photosystem II in flag leaves of two rice (*Oryza sativa* L.) cultivars that differ in their responses to nitrogen-deficiency, Plant Prod. Sci. 13 (2010) 11–20.
[19] C. Lu, J. Zhang, Q. Zhang, L. Li, T. Kuang, Modification of photosystem II photochemistry in nitrogen deficient maize and wheat plants, J. Plant Physiol. 158 (2001) 1423–1430.
[20] A. Carstensen, A. Herdean, S.B. Schmidt, A. Sharma, C. Spetea, M. Pribil, S. Husted, The impacts of phosphorus deficiency on the photosynthetic electron transport chain, Plant Physiol. 177 (2018) 271–284.
[21] S. Wieneke, M. Balzarolo, H. Asard, H. Abd Elgawad, J. Peñuelas, U. Rascher, A. Ven, M.S. Verlinden, I.A. Janssens, S. Vicca, Fluorescence ratio and photochemical reflectance index as a proxy for photosynthetic quantum efficiency of photosystem II along a phosphorus gradient, Agric. For. Meteorol. 322 (2022) 109019.
[22] H. Medrano, J.M. Escalona, J. Bota, J. Gulías, J. Flexas, Regulation of photosynthesis of C_3 plants in response to progressive drought: stomatal conductance as a reference parameter, Ann. Bot. 89 (2002) 895–905.
[23] J. Yang, S. Shuang, Z. Cun, J. Zhang, J. Chen, High nitrogen-driven photosynthesis limitation in shade-demanding species mediated by stomatal conductance through plasma membrane intrinsic proteins, Environ. Exp. Bot. 226 (2024) 105909.

[24] A.D.B. Leakey, J.N. Ferguson, C.P. Pignon, A. Wu, Z. Jin, G.L. Hammer, D.B. Lobell, Water use efficiency as a constraint and target for improving the resilience and productivity of C_3 and C_4 crops, Annu. Rev. Plant Biol. 70 (2019) 781–808.
[25] A.X. Liu, Photosynthesis Responses to Intrinsic Water Use Efficiency Depend on Atmospheric Feedbacks and Modify the Magnitude of Response to Elevated CO_2, University of Washington, 2024.
[26] K. Zhu, F.H. Yuan, A.Z. Wang, J.B. Wu, D.X. Guan, C.J. Jin, J. Flexas, C.J. Gong, H. X. Zhang, Y.S. Zhang, Stomatal, mesophyll and biochemical limitations to soil drought and rewatering in relation to intrinsic water-use efficiency in Manchurian ash and Mongolian oak, Photosynthetica 59 (2021) 49–60.
[27] H. Meidner, Light compensation points and photorespiration, Nature 228 (1970) 1349.
[28] D.N. Moss, E.G. Krenzer, W.A. Brun, Carbon dioxide compensation point in related plant species, Sci. Technol. Humanit. 164 (1969) 187–188.
[29] M.D. Fernández, Changes in photosynthesis and fluorescence in response to flooding in emerged and submerged leaves of *Pouteria orinocoensis*, Photosynthetica 44 (2006) 32–38.
[30] A.C. Franco, S. Matsubara, B. Orthen, Photoinhibition, carotenoid composition and the co-regulation of photochemical and non-photochemical quenching in neotropical savanna trees, Tree Physiol. 27 (2007) 717–725.
[31] B. Genty, J. Wonders, N.R. Baker, Non-photochemical quenching of F_o in leaves is emission wavelength dependent: consequences for quenching analysis and its interpretation, Photosynth. Res. 26 (1990) 133–139.
[32] A. Laisk, V. Oja, B. Rasulov, H.Y. Eichelmann, A. Sumberg, Quantum yields and rate constants of photochemical and nonphotochemical excitation quenching: experiment and model, Plant Physiol. 115 (1997) 803–815.
[33] M. Misumi, H. Katoh, T. Tomo, K. Sonoike, Relationship between photochemical quenching and non-photochemical quenching in six species of cyanobacteria reveals species difference in redox state and species commonality in energy dissipation, Plant Cell Physiol. 57 (2016) 1510–1517.
[34] K. Maseyk, T.B. Lin, A. Cochavi, A. Schwartz, D. Yakir, Quantification of leaf-scale light energy allocation and photoprotection processes in a Mediterranean pine forest under extensive seasonal drought, Tree Physiol. 39 (2019) 1767–1782.
[35] S. Shrestha, H. Brueck, F. Asch, Chlorophyll index, photochemical reflectance index and chlorophyll fluorescence measurements of rice leaves supplied with different N levels, J. Photochem. Photobiol., B 113 (2012) 7–13.
[36] C. Klughammer, U. Schreiber, Complementary PSII quantum yields calculated from simple fluorescence parameters measured by PAM fluorometry and the Saturation Pulse method, PAM Appl Notes 1 (2008) 27–35.
[37] D.M. Kramer, G. Johnson, O. Kiirats, G.E. Edwards, New fluorescence parameters for the determination of Q_A redox state and excitation energy fluxes, Photosynth. Res. 79 (2004) 209–218.
[38] C.R. Harris, K.J. Millman, S.J. van der Walt, R. Gommers, P. Virtanen, D. Cournapeau, E. Wieser, J. Taylor, S. Berg, N.J. Smith, R. Kern, M. Picus, S. Hoyer, M.H. van Kerkwijk, M. Brett, A. Haldane, J.F. del Río, M. Wiebe, P. Peterson, P. Gérard-Marchant, K. Sheppard, T. Reddy, W. Weckesser, H. Abbasi, C. Gohlke, T.E. Oliphant, Array programming with NumPy, Nature 585 (2020) 357–362.
[39] S. Jiao, W. Chen, J. Wang, N. Du, Q. Li, G. Wei, Soil microbiomes with distinct assemblies through vertical soil profiles drive the cycling of multiple nutrients in reforested ecosystems, Microbiome 6 (2018) 146.
[40] J.-W. Chen, S.-B. Kuang, G.-Q. Long, S.-C. Yang, Z.-G. Meng, L.-G. Li, Z.-J. Chen, G.-H. Zhang, Photosynthesis, light energy partitioning, and photoprotection in the shade-demanding species *Panax notoginseng* under high and low level of growth irradiance, Funct. Plant Biol. 43 (2016) 479–491.
[41] S. Ishida, K-i Morita, M. Kishine, A. Takabayashi, R. Murakami, S. Takeda, K. Shimamoto, F. Sato, T. Endo, Allocation of absorbed light energy in PSII to thermal dissipations in the presence or absence of PsbS subunits of rice, Plant Cell Physiol. 52 (2011) 1822–1831.
[42] O. Sherstneva, A. Khlopkov, E. Gromova, L. Yudina, Y. Vetrova, A. Pecherina, D. Kuznetsova, E. Krutova, V. Sukhov, V. Vodeneev, Analysis of chlorophyll fluorescence parameters as predictors of biomass accumulation and tolerance to heat and drought stress of wheat (*Triticum aestivum*) plants, Funct. Plant Biol. 49 (2022) 155–169.
[43] L. Hendrickson, R.T. Furbank, W.S. Chow, A simple alternative approach to assessing the fate of absorbed light energy using chlorophyll fluorescence, Photosynth. Res. 82 (2004) 73–81.
[44] G. Quero, V. Bonnecarrère, S. Fernández, P. Silva, S. Simondi, O. Borsani, Light-use efficiency and energy partitioning in rice is cultivar dependent, Photosynth. Res. 140 (2019) 51–63.
[45] N.R. Baker, Chlorophyll fluorescence: a probe of photosynthesis in vivo, Annu. Rev. Plant Biol. 59 (2008) 89–113.
[46] A. Porcar-Castell, E. Juurola, E. Nikinmaa, F. Berninger, I. Ensminger, P. Hari, Seasonal acclimation of photosystem II in *Pinus sylvestris*. I. Estimating the rate constants of sustained thermal energy dissipation and photochemistry, Tree Physiol. 28 (2008) 1475–1482.
[47] M. Knoblauch, W.S. Peters, Long-distance translocation of photosynthates: a primer, Photosynth. Res. 117 (2013) 189–196.
[48] L.S. Chen, L. Cheng, Both xanthophyll cycle-dependent thermal dissipation and the antioxidant system are up-regulated in grape (*Vitis labrusca* L. cv. Concord) leaves in response to N limitation, J. Exp. Bot. 54 (2003) 2165–2175.
[49] C.-M. Lu, J.-H. Zhang, Photosystem II photochemistry and its sensitivity to heat stress in maize plants as affected by nitrogen deficiency, J. Plant Physiol. 157 (2000) 124–130.
[50] P. Vijayalakshmi, T. Vishnukiran, B. Ramana Kumari, B. Srikanth, I. Subhakar Rao, K.N. Swamy, K. Surekha, N. Sailaja, L.V. Subbarao, P. Raghuveer Rao, D. Subrahmanyam, C.N. Neeraja, S.R. Voleti, Biochemical and physiological characterization for nitrogen use efficiency in aromatic rice genotypes, Field Crops Res. 179 (2015) 132–143.
[51] P.-M. Li, R.-G. Cai, H.-Y. Gao, T. Peng, Z.-L. Wang, Partitioning of excitation energy in two wheat cultivars with different grain protein contents grown under three nitrogen applications in the field, Physiol. Plantarum 129 (2007) 822–829.
[52] J. Jacob, D.W. Lawlor, *In vivo* photosynthetic electron transport does not limit photosynthetic capacity in phosphate-deficient sunflower and maize leaves, Plant Cell Environ. 16 (1993) 785–795.
[53] K.K. Niyogi, Photoprotection revisited: genetic and molecular approaches, Annu. Rev. Plant Physiol. Plant Mol. Biol. 50 (1999) 333–359.
[54] S.K. Singh, V.R. Reddy, Response of carbon assimilation and chlorophyll fluorescence to soybean leaf phosphorus across CO_2: alternative electron sink, nutrient efficiency and critical concentration, J. Photoch Photobiol. 151 (2015) 276–284.
[55] Q. Zheng, J. Hu, Q. Tan, H. Hu, C. Sun, K. Lei, Z. Tian, T. Dai, Improved chloroplast Pi allocation helps sustain electron transfer to enhance photosynthetic low-phosphorus tolerance of wheat, Plant Physiol. Biochem. (Issy les Moulineaux, Fr.) 201 (2023) 107880.
[56] B.S. Ripley, S.P. Redfern, J. Dames, Quantification of the photosynthetic performance of phosphorus-deficient *Sorghum* by means of chlorophyll-a fluorescence kinetics, South Afr. J. Sci. 100 (2004) 615–618.
[57] S.K. Singh, V.R. Reddy, D.H. Fleisher, D.J. Timlin, Relationship between photosynthetic pigments and chlorophyll fluorescence in soybean under varying phosphorus nutrition at ambient and elevated CO_2, Photosynthetica 55 (2017) 421–433.
[58] B. Jákli, E. Tavakol, M. Tränkner, M. Senbayram, K. Dittert, Quantitative limitations to photosynthesis in K deficient sunflower and their implications on water-use efficiency, J. Plant Physiol. 209 (2017) 20–30.
[59] X.F. Yang, Z.-L. Bie, J.L. Xu, Effects of potassium supply on the growth, photosynthetic characteristics and quality of lettuce, Acta Hortic. 761 (2007) 471–476.
[60] E. Garnier, J.-L. Salager, G. Laurent, L. Sonié, Relationships between photosynthesis, nitrogen and leaf structure in 14 grass species and their dependence on the basis of expression, New Phytol. 143 (1999) 119–129.
[61] J. Gong, Research on the Thickness of Wheat Leaves, Huaibei Normal University, 2014.
[62] T. Li, Y.-L. Li, Z.-Q. Li, C.-D. Jiang, L. Shi, Y.-J. Liu, Effects of leaf development on anthocyanin induced by high light and excited energy distribution in *Ocimum basilicum* L, Plant Physiol. J 50 (2014) 675–682.
[63] P.J. Franks, P.L. Drake, D.J. Beerling, Plasticity in maximum stomatal conductance constrained by negative correlation between stomatal size and density: an analysis using *Eucalyptus globulus*, Plant Cell Environ. 32 (2009) 1737–1748.
[64] J. Gago, C. Douthe, I. Florez-Sarasa, J.M. Escalona, J. Galmes, A.R. Fernie, J. Flexas, H. Medrano, Opportunities for improving leaf water use efficiency under climate change conditions, Plant Sci. 226 (2014) 108–119.
[65] J. Jacob, D.W. Lawlor, Stomatal and mesophyll limitations of photosynthesis in phosphate deficient sunflower, maize and wheat plant, J. Exp. Bot. 42 (1991) 1003–1011.
[66] M.M. Barbour, B.N. Kaiser, The response of mesophyll conductance to nitrogen and water availability differs between wheat genotypes, Plant Sci. 251 (2016) 119–127.
[67] D. Zhong, Y. Chi, J. Ding, N. Zhao, L. Zeng, P. Liu, Z. Huang, L. Zhou, Decoupling of nitrogen allocation and energy partitioning in rice after flowering, Ecol. Evol. 14 (2024) e11297.
[68] D. Wang, T. Ling, P. Wang, P. Jing, J. Fan, H. Wang, Y. Zhang, Effects of 8-year nitrogen and phosphorus treatments on the ecophysiological traits of two key species on Tibetan Plateau, Front. Plant Sci. 9 (2018) 1290.
[69] Y. Zheng, F. Li, L. Hao, A.A. Shedayi, L. Guo, C. Ma, B. Huang, M. Xu, The optimal CO_2 concentrations for the growth of three perennial grass species, BMC Plant Biol. 18 (2018) 27.
[70] Y. Zheng, F. Li, L. Hao, J. Yu, L. Guo, H. Zhou, C. Ma, X. Zhang, M. Xu, Elevated CO_2 concentration induces photosynthetic down-regulation with changes in leaf structure, non-structural carbohydrates and nitrogen content of soybean, BMC Plant Biol. 19 (2019) 255.
[71] E.H. Murchie, T. Lawson, Chlorophyll fluorescence analysis: a guide to good practice and understanding some new applications, J. Exp. Bot. 64 (2013) 3983–3998.